

Emil Omurzak

## EFFECT OF SURFACTANT MATERIALS ON FORMATION OF ZnO NANORODS UNDER IN-LIQUID PULSED PLASMA CONDITIONS

Эмил Омурзак

## ВЛИЯНИЕ ПОВЕРХНОСТНО-АКТИВНЫХ ВЕЩЕСТВ НА ФОРМИРОВАНИЕ ZnO НАНОСТРУКТУР В УСЛОВИЯХ ИМПУЛЬСНОЙ ПЛАЗМЫ В ЖИДКОСТИ

UDK: :547.495.5-148:661.

*Pulsed plasma generated by electrical discharge between two electrodes made of pure metallic zinc rods submerged into deionized water resulted in production of the hexagonal type ZnO nanostructures. Synthesized ZnO nanostructures were of rod shape with a diameter of about 20 nm and length up to 150 nm. Formation mechanism of ZnO nanorods was proposed on the basis of the atomic emission spectroscopy and the microscopic analyses.*

*Pulsed plasma in surfactant solutions such as positively-charged cetyltrimethylammonium bromide (CTAB) and negatively-charged sodium dodecyl sulfate (SDS) induced formation of pure ZnO, while non-ionic octaethylene glycol monododecyl ether (OGM) and zwitter-ionic sulfobetain (SB) resulted in a mixture of ZnO with Zn. Also, morphology of formed nanorods were different from each other for each surfactant, particularly, negatively charged surfactant SDS caused formation of larger in terms of length-to-diameter ratio ZnO nanorods than that of the positively charged surfactant CTAB.*

*Синтезированы наноструктуры оксида цинка из чистого цинка с применением импульсной плазмы в деионизированной воде. Полученные наноструктуры имеют форму наностержней с диаметром примерно 20 нм и с длиной до 150 нм. Механизм формирования наностержней оксида цинка был предложен на основании атомно-эмиссионной спектроскопии плазмы и микроскопических анализов полученных образцов.*

*Влияния растворов поверхностно активных веществ (ПАВ) с разными полярностями на формирование наноструктур ZnO было выявлено, например, положительно заряженный цетилтриметиламмоний бромида (ЦТМБ) и негативно-заряженный додецилсульфат натрия (ДСН) способствовали формированию чистого ZnO, а применение без-ионного octaethyleneglycolmonododecylether (OGM) и циттер-ионного сульфобетаина (СБ) привело к созданию смеси оксида и металлического цинка. Морфология полученных наностержней были разными для каждого ПАВ, в частности, негативно заряженный ДСН способствовал появлению наностержней с более крупными размерами (соотношение длины к диаметру) чем в случае с позитивным ЦТМБ.*

## Introduction

ZnO is a transition metal oxide semiconductor and recognized as an important material for various applications. It has wide band-gap energy equal to 3.37 eV and a large exciton binding energy of 60 meV. Zinc oxide normally forms in the hexagonal (wurtzite) crystal structure and is a unique material that exhibits optical, photocatalytic, piezoelectric properties. ZnO has been used as solar cells, luminescent devices [1], phosphor material for flat panel displays [2] and a photocatalyst [3,

4]. Well-dispersed ZnO nanoparticles with large surface area can provide additional benefits of higher efficiency.

There have been reported various method for synthesis of zinc oxides such as sol-gel method [5], hydrothermal synthesis [6-10], using supercritical water [11], microwave plasma [12], electro-chemical deposition technique [13], and dc thermal plasma [14-16]. The references from 14 to 16 described the same method that produced particles of micron order with specific surface area of 7 to 15 m<sup>2</sup>/g, which is quite small. Gas-sensor made of nano-ZnO prepared by arc plasma method was reported [17], in which nanoparticles of metallic zinc were prepared at first, and then these particles were subjected to thermal treatment in air at 300 and 600 °C that resulted in zinc oxide particles of 60 and 200 nm respectively. In addition, effect of surfactant materials to the formation of the ZnO nanostructures has not been studied in details.

Here we report preparation of ZnO nanorods by the pulsed plasma in liquid method [18, 19], which is a combination of physical (spark discharge) and chemical processes (surrounding liquid) that provide us a number of advantages (simple, one-step, low-energy, versatile) for the synthesis of various kinds of metastable nanomaterials. And effect of the surfactant materials with different polarity to the formation of the zinc oxide nanomaterials was studied.

## Experimental Procedure

The experimental procedure is described in ref. 19. For this experiment, rod shaped electrodes with diameters of 5 mm and length of 100 mm made from 99.9 % purity zinc were used. The electrodes were submerged about 5-7 cm deep into the deionized water in 200 ml beaker and fixed in the form of V. Duration of a single discharge was measured to be about 10 μs and peak current about 100 A. After that the pulsed plasma was applied for an hour. Increase of the liquid temperature during the experiment was insignificant (after 1 h of continuous applying of the electrical discharge, temperature increase was about 5 K) due to the short duration of the pulsed discharge and thus no need for cooling of electrodes and/or liquid. The formed powder was separated from water by centrifuge and then was dried in air at 110 °C by using a muffle furnace.

For studying the effect of surfactant materials on formation of ZnO, 4 kinds of surfactants with different polarity were used: cetyltrimethyl ammonium bromide (CTAB), sodium dodecyl sulfate (SDS), octaethylene glycol monododecyl ether (OGM), sulfobetaine 3-14 (SB). The details are given in the table I. The surfactant

material with concentration of 0.01mol/L was added to deionized water and stirred for about an hour, and then this solution was used for the experiment with continuous stirring throughout the experiment.

X-Ray Diffraction (XRD) patterns of the samples were taken using Cu K $\alpha$  radiation, Rigaku RINT-2500VHF. High Resolution Transmission Electron Microscopy (HRTEM) images of the products were taken by Philips Tecnai F20 S-Twin: some amount of

sample was dispersed in ethanol and then was taken by pipette and dropped on the copper grids (200 mesh).

Atomic emission spectrum of the plasma during the experiment was taken by using the SEC2000 spectrophotometer capable of capturing wavelength between 200 - 900 nm with a resolution of  $\approx$  2.3 nm; slit 50  $\mu$ m x 1000  $\mu$ m. Quartz beaker of 200 ml was used in order to avoid UV range wavelength cut off.

**Table I.** List of surfactant materials used for our experiments.

<i>Abbr.</i>	<i>Name of surfactant</i>	<i>Charge</i>
CTAB	Cetyltrimethylammoniumbromide	Cationic (+)
SDS	Sodiumdodecylsulfate	Anionic (-)
OGM	Octaethylene Glycol Monododecyl Ether	Non-ionic
SB	Sulfobetaine 3-14	Zwitterionic (+-)

## Results and Discussions

### 1. Crystal structure, morphology and formation mechanism

Figure 1a represents the XRD pattern of the synthesized sample produced by the pulsed plasma between two zinc electrodes submerged in water. Phase composition of the sample was determined to match with the JCPDS card No. 65-3411, which is hexagonal zinc oxide. Refined lattice parameters of produced ZnO were a=3.255 and c=5.217 Å; whereas JCPDS powder diffraction file (65-3411) has 3.25 and 5.207 Å, respectively. The plasma-process produced ZnO possesses slightly larger cell parameters. This can be related to the non-equilibrium state of plasma zone, where the crystals are formed. In addition to the ZnO phase, there were also peaks that belong to metallic zinc.

TEM images of the sample are given in the Figure 1b and 1c. We can see that the particles are mostly in rod shape with a diameters ranging from 10 to 50 nm. Majority of ZnO nanorods were assembled into bush-like aggregates. However, separated nanorods were also observed (Fig. 1c). The lengths of the nanorods are from 20 to 150 nm.

Figure 2 displays the atomic emission spectrum of the plasma generated by the pulsed electric discharge between zinc electrodes in water and the formation mechanism of ZnO nanorods with insets of HRTEM images of the sample. The identification of the spectral lines was done using the online database [20]. The peaks belonging to Zn and O atoms in neutral and ionized states were identified. This emission is generated by passage of high current across the inter-electrode space by breaking the potential difference as a result of ionization process due to the electrical field between the electrodes. This breakdown evaporates the surface of the electrode and creates the vapor from electrode material. At the same time the water splits into ions of oxygen, hydrogen, OH radicals and so on, which will participate in the formation of the zinc oxide nanocrystals. This step towards the formation of zinc oxide nanostructures is illustrated in Fig. 2 (1). Ions from the evaporated raw materials (Zn and water) will react with each other to form ZnO nanocrystals, which will serve as “seeds” for the growth of ZnO nanorods (Fig. 2 (2)). The inset of (2) shows the HRTEM image of a single crystal ZnO quenched in early stage of formation due to the non-equilibrium state of the pulsed plasma and grown from spontaneous nucleation process.

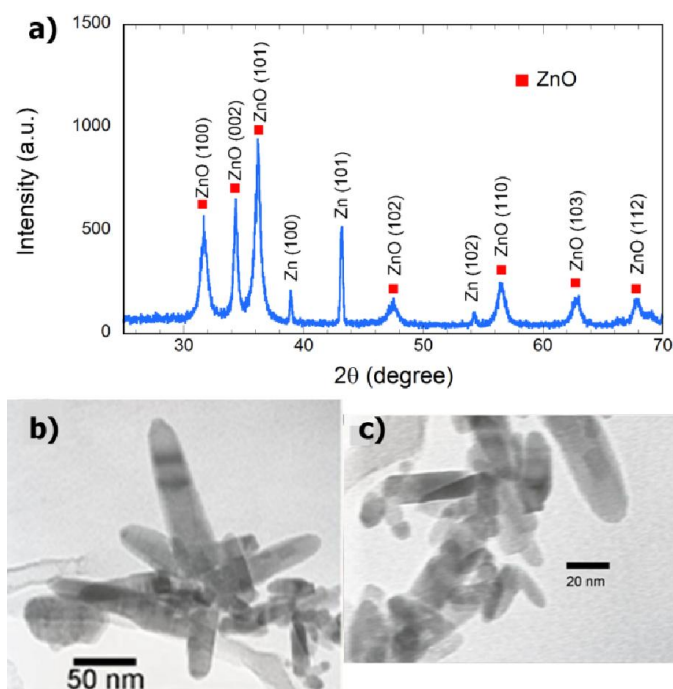


**Fig. 1.** a) XRD pattern of the synthesized sample by the pulsed plasma between two zinc electrodes submerged in water. Each peak is labeled with the identified lattice plane of ZnO or Zn. b) and c) TEM images of the synthesized sample.

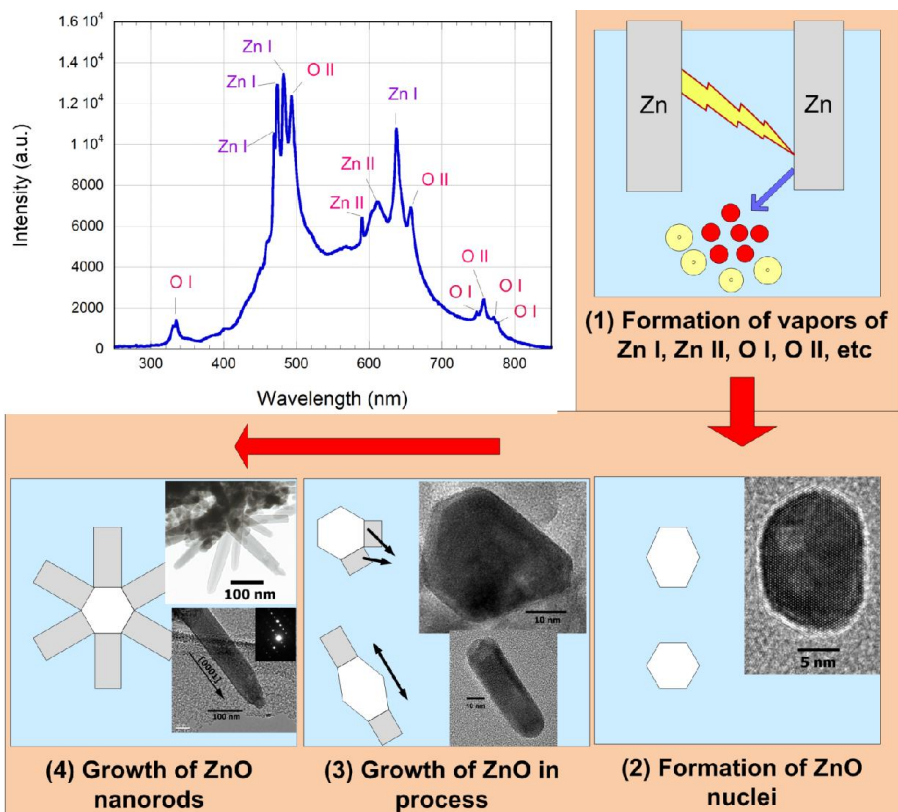


**Fig. 2.** Atomic emission spectrum of the plasma generated by the pulsed electric discharge between zinc electrodes in water and the formation pathway of the ZnO nanorods with insets of HRTEM images of the sample.

**Fig. 2 (3)** shows the starting the growth of the nanorod structures from the single crystals, some of the hexagonal structures started to stretching out from some of planes of ZnO crystal in some directions. Finally, growth of nanorod structure up to 150 nm is followed, as exhibited in (4). The nanorods grew in [0001] direction, i.e. along the c axis, which was confirmed by the selected area electron diffraction (SAED) pattern for the structure (see the inset of (4)). The growth direction of the ZnO nanorods was reported in ref. [6, 10], which indicate that the ZnO nanorods grow in the [0001] direction.

## 2. Effect of surfactants

Figure 3 displays the comparison of XRD patterns of the samples produced in different surfactant solutions with that of without surfactant. The arrows denote the diffraction angles positions, where the prominent peaks belonging to metallic zinc reflect (39, 43, 54 °). As we can see, the sample produced without surfactant had high intensity peaks at 39, 43, 54 degrees, indicating the presence of metallic zinc content. Similar results were elaborated when non-ionic and zwitter-ionic surfactants were used. But, in case of cationic and anionic surfactants, the peak intensity belonging to zinc dropped significantly or almost disappeared from the XRD patterns. This suggests that using the charged surfactant, whether negatively or positively, would be favorable for growth of pure ZnO nanorods under the pulsed plasma in water conditions. More discussions are given in coming paragraphs below.

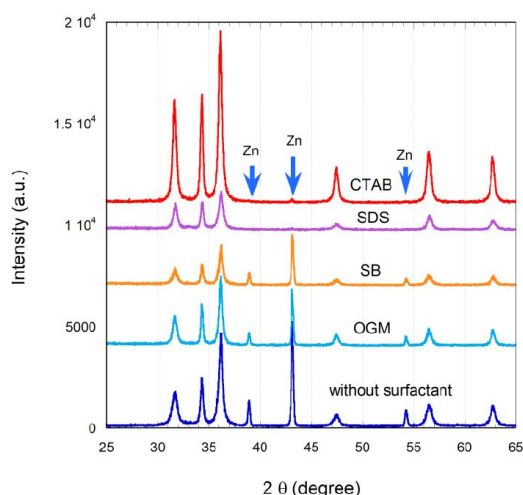


**Fig. 3.** XRD patterns of the samples produced by the pulsed plasma using zinc electrodes submerged in different surfactant solutions. The arrows denote the diffraction angles positions, where the prominent peaks belonging to metallic zinc reflect.

If we look at the microscopic images, shown in Figure 4, of the samples produced by using different surfactant materials, we can see that their morphologies are different from each other in terms of diameter and length of the nanorods. In order to qualitatively describe the difference between the morphologies of the nanorods, size distribution was determined.

Figure 5 shows distributions of length and diameter of the samples prepared by using CTAB, SDS, OGM and SB. Fig. 5 a, c, e, g displays the distribution of nanorod length for CTAB, SDS, OGM, SB, respectively. Distribution was determined by using the FE-SEM images of the samples on the image processing software. Average length of the nanorods for CTAB and OGM were similar and equal to about 120 nm, while that of SDS was more than double of this value (246 nm). For the case of SB, the nanorod growth was really poor, instead it resembled a bid aggregated particle on the surface of which some short nanorod structures grew. The diameter of the nanorods produced using these four kinds of surfactant materials also differ. Fig. 5(b, d, f, h)

display the distribution of the diameter of the nanorods prepared in different kinds of surfactants. Here also the CTAB and OGM samples showed similar size of nanorod diameters, which was 28 and 26 nm, respectively. While that of SDS was the double of this diameter and equaled to 55 nm. OGM showed the smallest diameter, but since the nanorods were poorly grown, we can disregard this value.



**Fig. 4.** (a-d) FE-SEM images of the produced ZnO samples by using different kinds of surfactant materials. The images were taken at similar magnification and thus the scale bars in the images are same and equal to 100 nm. e) Schematic illustration of possible interaction between the Zn ions and the surfactant materials during the formation process.

Fig. 4e displays the interaction between the Zn ion and the surfactant materials hydrophilic head. Atomic emission spectroscopy of the pulsed plasma between zinc electrodes submerged in water confirmed the generation of neutral and positive Zn atoms. We considered that Zn ion will take significant role in interaction with the charged heads of surfactant materials. Accordingly, the strong interaction or reaction between the Zn ion and the surfactants could cause significant change in the formation of ZnO nanorods. This is clearly evident from the XRD pattern of the samples prepared using the SDS and CTAB, which were purely ZnO phase. In other words, the strong interaction between the CTAB/SDS and the Zn ion suppressed aggregation of zinc atoms into bigger particles. As a result pure zinc oxide nanorods were grown. Similar results were achieved by the laser ablation of zinc plate in surfactant solutions of lauryl dimethylaminoacetic acid (LDA) and CTAB [21]. Although they used higher temperature aqueous medium (80 °C) than in our case (room temperature), the results were similar for CTAB. And they related this phenomenon to the strong interaction that inhibits adsorption of Zn species on the surface of ZnO particle and induce the growth even more.

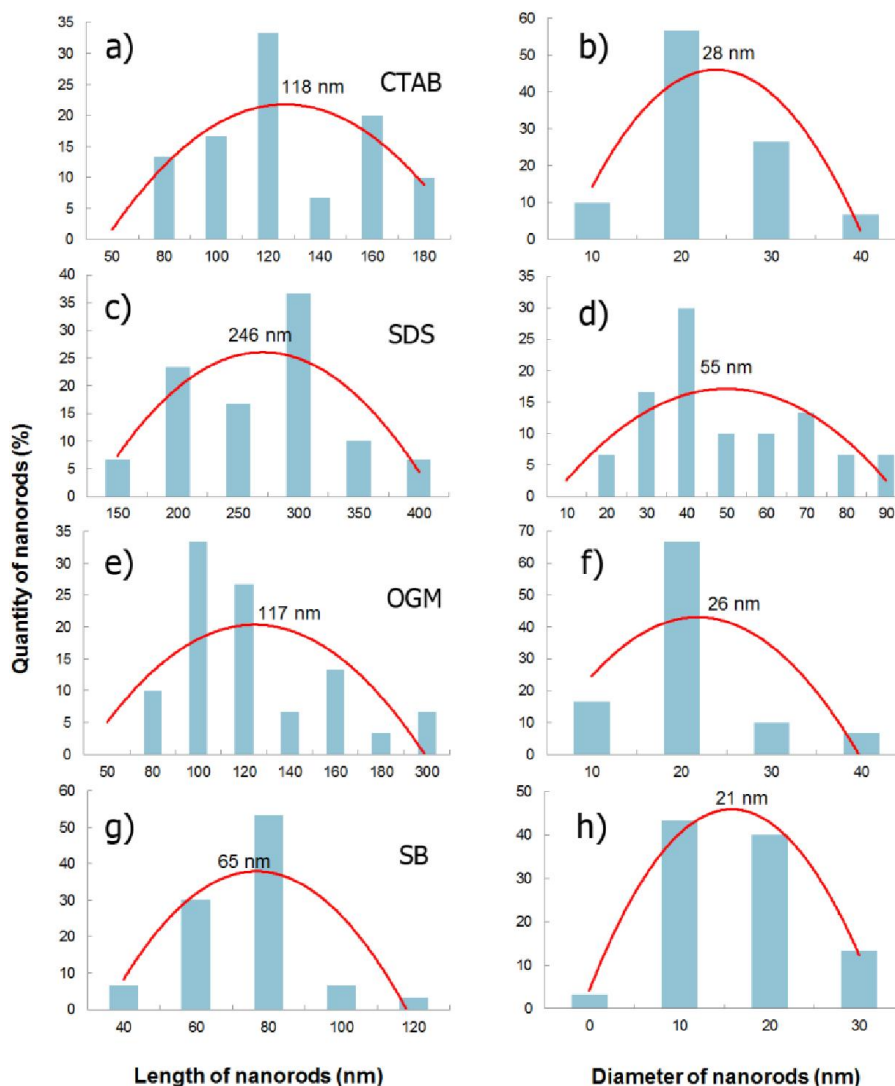


Fig. 5. Distribution of diameters and lengths of the ZnO nanorods prepared using different kinds of surfactants: (a, b) CTAB, (c, d) SDS, (e, f) OGM, (g, h) SB.

Polarity of the surfactants also materializes in crystallinity of the final product, i.e. ZnO nanorods. Crystallinity of the samples, estimated from the XRD peak intensities (Fig. 5), decreased when the surfactant materials were added except the case of CTAB, which in contrary induced the better crystallinity of the ZnO nanorods.

#### Summary

We have synthesized hexagonal ZnO nanostructure with about 20 nm in diameter by the pulsed plasma between two zinc electrodes submerged into deionized water. Phase composition of the sample was determined to match with the hexagonal ZnO with JCPDS card No. 65-3411 and the lattice parameters of the synthesized by this method ZnO were slightly larger than that of the card data. TEM observation showed that the synthesized ZnO sample was in nanorod shape with an average diameter of about 20 nm and the length up to 150 nm. The growth direction of the nanorods was in the direction of c-axis, i.e. [0001] direction. Formation mechanism of ZnO

nanorods was proposed on the basis of atomic emission spectroscopy and microscopy analyses.

Effect of four kinds of surfactant materials with different polarity was studied: positively (CTAB) and negatively (SDS) charged surfactants induced formation of pure ZnO nanorods. In addition, SDS caused formation of larger ZnO nanorods compared to that of CTAB, which was related to the strong interaction between negative SDS head and the positive Zn ion that induced adsorption of more Zn atoms for faster growth of ZnO nanorods. The length, diameter and surface state of the nanorods were different when we use different surfactants: nanorods produced using SDS have rough surface, large diameter and short length, while nanorods formed under CTAB conditions exhibit smooth surface, smaller diameter and longer length.

#### Reference

1. W.C. Shih and M.S. Wu, "Growth of ZnO films on GaAs substrates with a SiO<sub>2</sub> buffer layer by RF planar magnetron sputtering for surface acoustic wave

- applications", *Journal of Crystal Growth*, 137 (1994), 319-325.
2. K. Vanheusden et al., "Green photoluminescence efficiency and free-carrier density in ZnO phosphor powders prepared by spray pyrolysis", *Journal of Luminescence* 75 (1997), 11-16.
  3. C.D. Jaeger and A.J. Bard, "Spin trapping and electron spin resonance detection of radical intermediates in the photodecomposition of water at titanium dioxide particulate systems", *Journal of Physical Chemistry*, 83 (1979), 3146-3152.
  4. R. Cai, K. Hashimoto and A. Fujishima, "Conversion of photo-generated superoxide anion into hydrogen peroxide in TiO<sub>2</sub> suspension system", *Journal of Electroanalytical Chemistry*, 326 (1992), 345-350.
  5. R.J. Lauf and W.D. Bond, "Fabrication of high-field zinc oxide varistors by sol-gel processing", *American Ceramics Society Bulletin*, 63 (1984), 278-281.
  6. B. Lin and H. C. Zeng, "Hydrothermal Synthesis of ZnO Nanorods in the Diameter Regime of 50 nm", *Journal of American Chemical Society*, 125 (2003), 4430-4431.
  7. H. Nishizawa, T. Tani and K. Matsuoka, "Crystal Growth of ZnO by Hydrothermal Decomposition of Zn-EDTA", *Journal of the American Ceramic Society*, 67 (1984), C-98-C-100.
  8. A. Chittofrati and E. Matijevic, "Uniform particles of zinc oxide of different morphologies", *Colloids and Surfaces*, 48 (1990), 65-78.
  9. C.H. Lu and C.H. Yeh, "Influence of hydrothermal conditions on the morphology and particle size of zinc oxide powder", *Ceramics International*, 26 (2000), 351-357.
  10. L. Xu et al., "ZnO with Different Morphologies Synthesized by Solvothermal Methods for Enhanced Photocatalytic Activity", *Chemistry of Materials*, 21 (2009), 2875-2885.
  11. K. Sue et al., "Continuous synthesis of zinc oxide nanoparticles in supercritical water", *Green Chemistry*, 5 (2003), 659-662.
  12. A. Irzh et al., "Synthesis of ZnO and Zn Nanoparticles in Microwave Plasma and Their Deposition on Glass Slides", *Langmuir*, 26 (2010), 5976-5984.
  13. M.J. Zheng et al., "Fabrication and optical properties of large-scale uniform zinc oxide nanowire arrays by one-step electrochemical deposition technique", *Chemical Physics Letters*, 363 (2002), 123-128.
  14. H.F. Liu, S.C. Liao, and S.W. Hung, "The dc thermal plasma synthesis of ZnO nanoparticles for visible-light photocatalyst", *Journal of Photochemistry and Photobiology A: Chemistry*, 174 (2005), 82-87.
  15. T.S. Ko et al., "ZnO nanoparticles fabricated by dc thermal plasma synthesis", *Materials Science and Engineering: B*, 134 (2006), 54-58.
  16. S.C. Liao et al., "dc thermal plasma synthesis and properties of zinc oxide nanorods", *Journal of Vacuum Science & Technology B*, 24 (2006), 1322-1327.
  17. L.F. Dong, Z.L. Cui and Z.K. Zhang, "Gas sensing properties of nano-ZnO prepared by arc plasma method", *Nanostructured Materials*, 8 (1997), 815-823.
  18. E. Omurzak et al., "Synthesis of Blue Amorphous TiO<sub>2</sub> and Ti<sub>2</sub>O<sub>3</sub> by the Impulse Plasma in Liquid", *Journal of Nanoscience and Nanotechnology*, 9 (2009), 6372-6375.
  19. E. Omurzak et al., "Synthesis Method of Nanomaterials by Pulsed Plasma in Liquid", *Journal of Nanoscience and Nanotechnology*, 7 (2007), 3157-3159.
  20. Kramida, A., Ralchenko, Yu., Reader, J., and NIST ASD Team (2012). *NIST Atomic Spectra Database* (ver. 5.0), [Online].
  21. Y. Ishikawa, Y. Shimizu, T. Sasaki, N. Koshizaki. "Preparation of zinc oxide nanorods by pulsed laser in water media at high temperature", *J. Colloid. Interface Sci.*, 300 (2006), 612-615.

Рецензент: к.х.н. Жаснакунов Ж.К.